Int. J. Electrochem. Sci., 13 **(2018)** 6259 – 6271, doi: 10.20964/2018.07.47

International Journal of
ELECTROCHEMICAL
SCIENCE
www.electrochemsci.org

Nitrogen-Phosphorus co-doped Porous Carbon Based on Peanut Shell for Surpercapactior

Jing Wang[1], *Yufan Li*[1], *Lei Yan*[1], *Yuning Qu*[2,*]

[1] Tianjin Key Laboratory of Advanced Fibers and Energy Storage, College of Materials Science and Engineering, Tianjin Polytechnic University, 399 Binshui West Road, Tianjin 300387, P. R. China
[2] College of Environment and Chemical Engineering, Tianjin Polytechnic University
[*]E-mail: quyuning@tjpu.edu.cn

Received: 3 April 2018 / *Accepted:* 5 May 2018 / *Published:* 5 June 2018

In this work, a porous carbon (PC) material derived from the peanut shell, with a fluffy structure, is activated by phosphorus (P-PC) or nitrogen and phosphorus (N,P-PC) using phosphoric acid and urea precursors, followed by pyrolysis in nitrogen atmosphere. The P doping or N,P co-doping are found to decrease the charge transfer resistance, facilitate the formation of a hierarchical porous structure and increase the graphitization degree. The morphology and characteristics of the modified PC materials are investigated by SEM, XRD and XPS together with electrochemical characterizations. As a result, among the P- PC samples the one with a doping ration 1:11 displays the highest specific capacitance (SC) of 284.8 F/g at the scan rate of 5 mV s^{-1} while among the the N,P-PC samples, the one with 1:2 ratio shows the highest SC of 330.8 F/g at the scan rate of 5 mV s^{-1} and 131.3 F/g at the current density of 1 A/g.

Keywords: Biomass, Co-doping, Supercapacitor, Specific capacitance

1. INTRODUCTION

Supercapacitors are a kind of energy storage devices in between the traditional capacitors and secondary batteries which has received increasing interest because of the high power density and excellent cycle-life [1-4]. With the increasing demand of high energy density, investigations on carbon-based materials [5,6] and different electrolytes [7,8] have attracted great attention. The energy density is well known to be calculated by the formula $E=½CV^2$, meaning that the performance of a supercapacitor can be increased both by increasing its capacitance or its working voltage.

Among carbon-based capacitors, activated carbon (AC) [9] with low cost and high surface area has been commonly used as electrode material. However, the inappropriate and blocked pore texture limits its performance and hindered their commercialization [10]. In order to enhance the

charge/discharge rate and the ion transport rate one could use two-dimensional (2D) materials and open porous carbon electrode materials [11]. Graphene, with its unique 2D surface and high in plane electrical conductivity has shown superior power-energy combination respect to ACs [12,13]. However, compared with AC, the high complexity of the processing technology [14-18] and high cost of graphene leads to a lack of competitiveness [19,20].

Heteroatom-doping is another way to decrease charge transfer resistance, thereby enhancing the capacitive performance of supercapacitors [21-24]. Carbon materials can be doped with heteroatoms such as nitrogen (N), oxygen (O), sulfur (S), boron (B) or phosphorus (P) in either a single- or binary-doping to modify its surface or bulk properties. Due to synergetic effect [25-27], binary-doped carbon materials allow achieving better performance than with single-doping with an heteroatom. In particular, S,N co-doping of graphene oxide (GO) was realized by Xu via chemical vapor deposition (CVD) method, allowing to control the S/N ratio [28]: the as-prepared co-doped graphene showed better performance than that other N-doped carbon materials. Fan [29] studied the N,S co-doping of porous carbon (PC) derived from willow catkin; the as-prepared carbon materials showed a unique cross-linked laminar structure and high specific capacitance (SC) of 298 F g^{-1} at 0.5 A g^{-1} and 233 F g^{-1} and 50 A g^{-1}. Phosphorus has similar properties than N, however P-doping could provide not only for a higher electron-donating ability but also for a larger atomic radius which may improve the electrocatalytic activity [30,31]. P,S co-doped carbon was synthesized using resorcinol and furaldehyde as carbon sources through sol-gel processing; the SC of such P,S-PC could reach up to 103.5 F g^{-1} [32]. Converting waste biomass into biofuels and bioderived materials rather than incineration is a pressing environment need [33].

In this work, we use peanut shell as waste biomass carbon source, mainly consisting of cellulose, lignin and hemicelluloses. Porous carbon materials derived from peanut shell carbonization display high porosity and form single peak or multi peak pore size distribution, which can effectively improve the ionic permeability and conductivity of electrode materials. After P-doping or N,P-co-doping, the carbonized precursor gains a porous structure. The morphology and electrochemical characteristics are investigated in details.

2. MATERIALS AND METHODS

2.1. Materials

Peanut shell was obtained from a peanut mill nearby Tianjin. Peanut shell was shredded into pieces about 0.5 cm^2 and washed with deionized water. Finally, the pieces were dried at 120 ^oC overnight. Phosphoric acid (H_3PO_4), potassium hydroxide (KOH) and carbamide ($CO(NH_2)_2$) were all of analytical grade (Tianjin Guangfu Fine Chemical Research institute, AR).

2.2. Preparation of Phosphorus-doped porous carbon (P-PC) and Nitrogen-Phosphorus co-doped Porous Carbon (N,P-PC)

Peanut shell pieces were activated with phosphoric acid (50%) with the ratio of the peanut shell weight to the phosphoric acid volume of 1:8, 1:9, 1:10, 1:11 and 1:12. After 12 h, the mixture was

dried at 120 ^{o}C for 10 h and then activated at 500 ^{o}C for 1 h. The obtained product was washed with deionized water until neutral. Finally, the compound was carbonized at 800 ^{o}C in a furnace with nitrogen atmosphere for 2 h and then grinded to get P-PC. N,P-PC was obtained in a similar way. For the selected P-PC 1:11, carbamide was used as nitrogen source to dope N into the P-PC matrix. N,P-PCs were obtained by phosphoric acid after pyrolysis of N-doped activated carbon/carbamide samples with mass ratio of 1:1 to 1:4.

2.3. Materials characterization

Field-emission scanning electron microscopy (FE-SEM, Hitachi S-4800) and high-resolution transmission electron microscopy (HR-TEM, Tecnai G2 F20) were taken to observe the morphology and structure of PCs. X-ray diffraction (XRD) was carried out on a Rigaku D/Max2500 X-ray diffractometer using Cu Kαradiation. The surface chemical composition was investigated by X-ray photoelectron spectroscopy (XPS).

.

2.4 Electrochemical Measurement

Galvanostatic charge/discharge (GCD), electrochemical impedance spectroscopy (EIS) were taken in 6M KOH electrolyte solution by using a three-electrode system. Arbin USA used for GCD tests were performed at current density ranging from 1 to 10.0 A/g. EIS (Autolab PGSTAT128N, Switzerland) plots were acquired in the frequency range from 100 kHz to 1 mHz at an AC amplitude of 0.005 V. Cyclic voltammetry (CV) curves (CHI604D, China) were acquired at scan rates from 5 to 1000 mV /s. Followed the equation, the specific capacitance was calculated as $C_m=2I\triangle t/m\triangle V$, where I, $\triangle t$, $\triangle V$ and m was the discharge current, discharge time, the voltage window and active material mass of the single electrode. Followed the equation, the specific capacitance was calculated as $Cm=2I\triangle t/m\triangle V$, where I, $\triangle t$, $\triangle V$ and m was the discharge current, discharge time, the voltage window and active material mass of the single electrode.

3. RESULTS AND DISCUSSION

3.1. Characterizations of the P-PC and N,P-PC samples

P-PC and N,P-PC are fabricated via a simple high temperature carbonization process by using phosphoric acid and urea as activating agents, as depicted in Scheme 1. Figure 1 shows the SEM and HR-TEM images of P-PC and N,P-PC samples indicating a non-uniform particle size distribution (Figure 1a and 1b). After the activation, a hierarchical porous structure is observed mainly consisting of micro- and meso- pores (Figure 1c and 1d). Meanwhile, small randomly-distributed disordered graphite crystallites are seen. XRD patterns of P and N,P doped materials are shown in Figure 2. Both samples display the same characteristic peaks with a broad diffraction peak at $2\theta=23.6^{o}$ is ascribed to

the presence of amorphous carbon structures and graphene (002), and a the weaker diffraction peak at 43.8^{o} demonstrating the presence small graphite (100) crystallites [34,35].

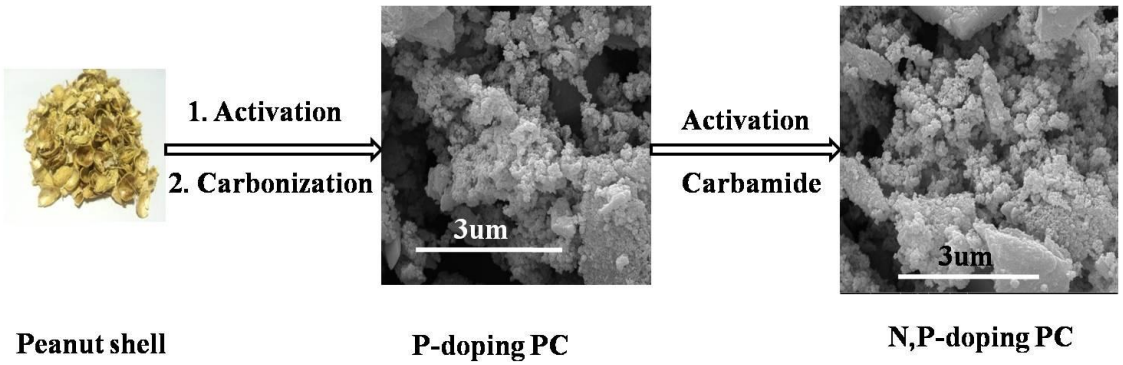

Scheme 1. Schematic diagrams illustrating the preparation process of N-PC and N,P-PC samples.

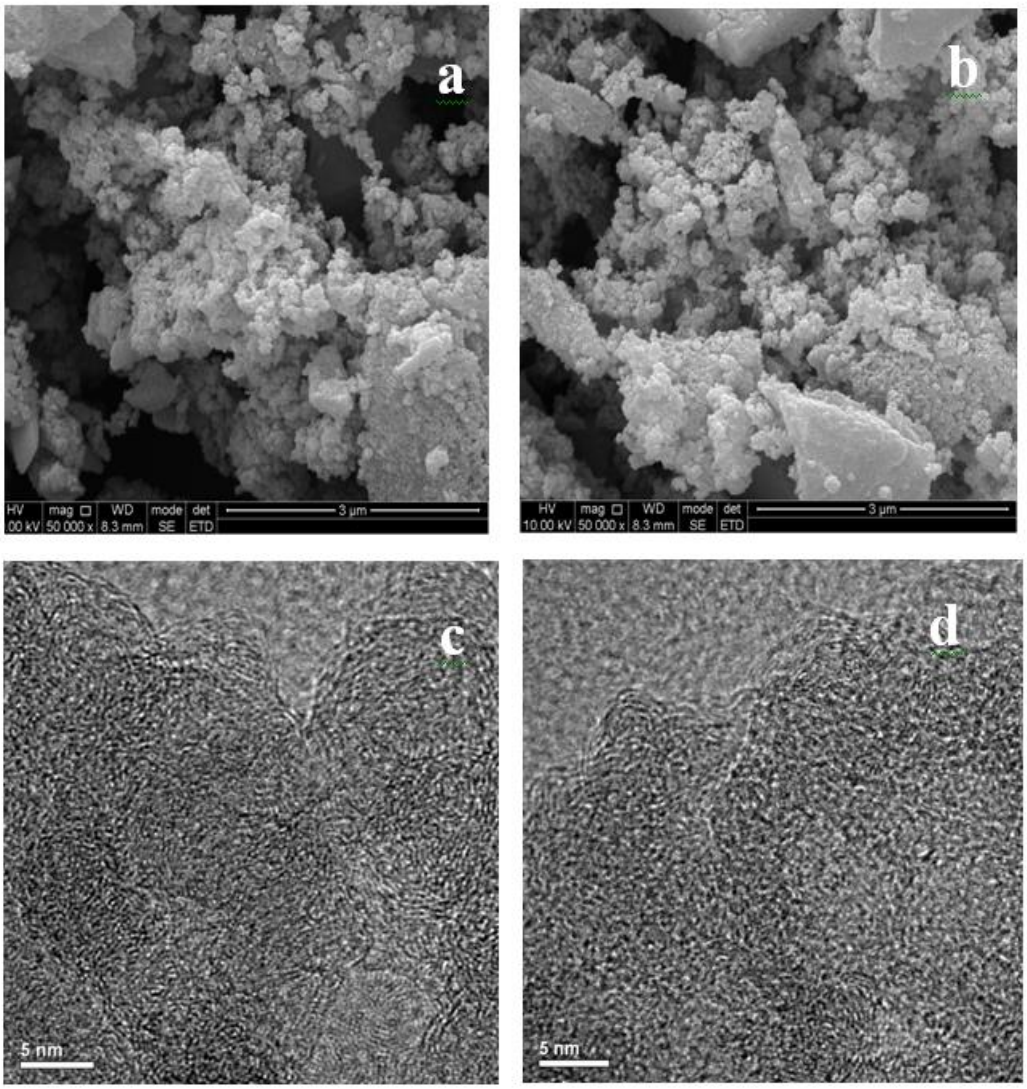

Figure 1. SEM images of (a) P-PC (1:11), (b) N,P-PC (1:2) and HR-TEM images of (c) P-PC (1:11) and (d) N,P-PC (1:2).

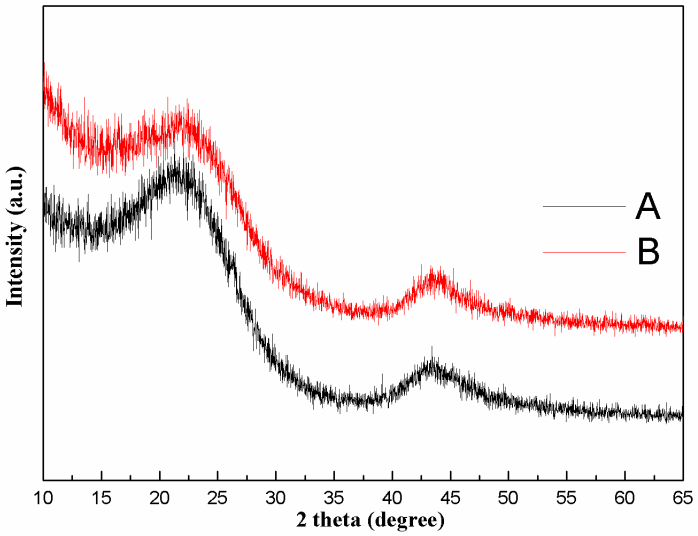

Figure 2. XRD patterns of (a) P-PC (1:11), (b) N,P-PC (1:2).

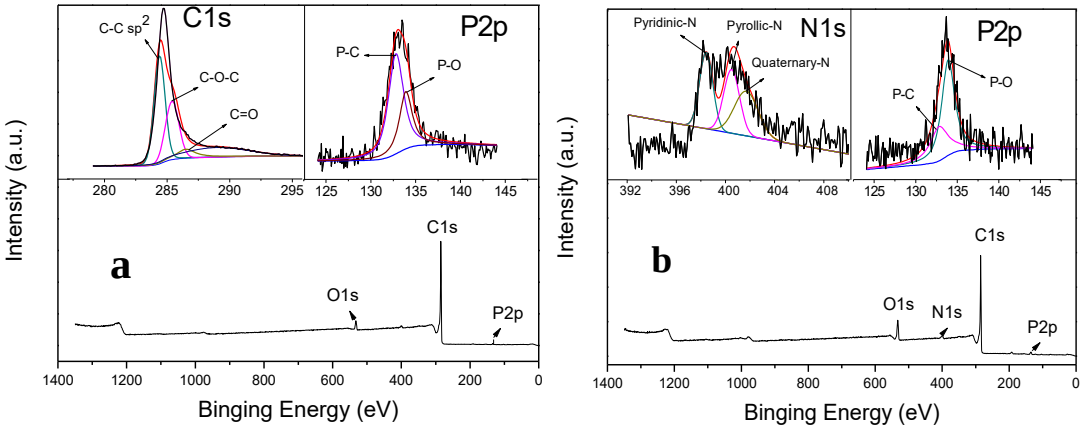

Figure 3. XPS spectra of (a) P-PC (1:11), (b) N,P-PC (1:2).

XPS analysis was performed o characterize the surface properties of the P-PC and N,P-PC samples (Figure 3). Both survey and high-resolution P 2p, C 1s, and O 1s spectra have been analyzed. Three peak components identified in the C 1s spectrum (Fig. 3a) centered at the binding energy of 284.6, 285.4 and 286.5 eV are ascribed to C-C sp2, C-O-C and C=O, respectively [36]. Meanwhile, the P 2p spectrum is fitted with two components at the binding energy of 132.8 and 133.9 eV representing P-C and P-O bondings, respectively [37,38]. Overall the results indicate that P is successfully inserted into the porous carbon and that graphite crystallites are present within the structure. As shown in Figure 3b, the survey spectra allow identifying and quantifying N 1s, P 2p, C 1s and O 1s elements. The N 1s spectrum is fitted with three components at 398.4, 400.4 and 401.5 eV binding energy corresponding to pyridinic, pyrrolic and graphitic N, respectively. The pyrrolic and graphitic N may yield to pseudocapacitance effects [39], promoting the electrochemical performance of the capacitor.

3.2. Electrochemical performance

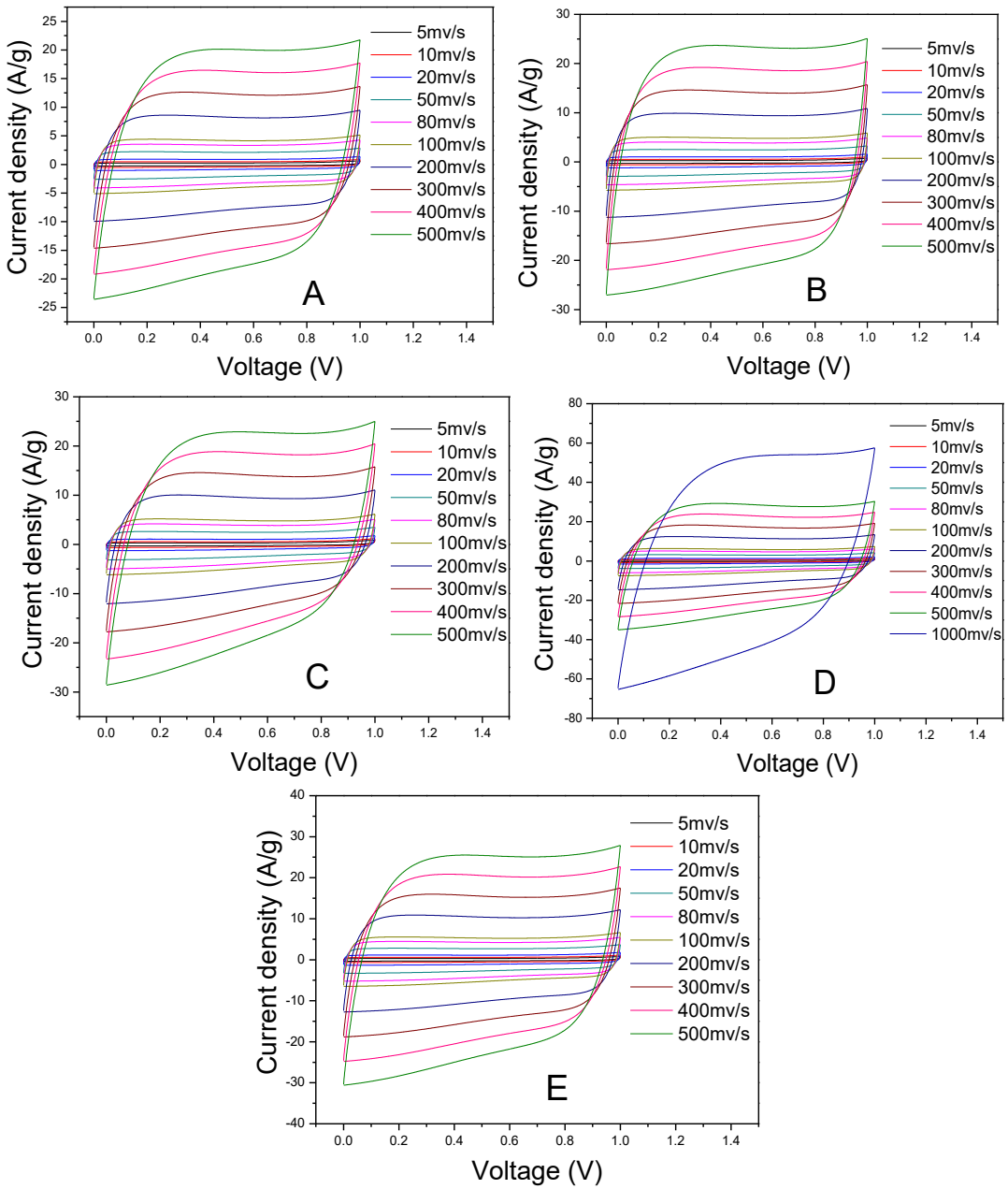

Figure 4. CV curves of P-PCs (a) 1:8, (b)1:9, (c)1:10 and (e) 1:12 at the scan rate between 5 and 500 mV/s and (d)1:11 at the scan rate between 5 and 1000 mV/s within the operating voltage of 0-1 V in 6 M KOH.

Figure 4 and 6 show the CV curves of P-PC and N,P-PC electrodes at different sweep speeds (5-500 mV/s) in 6 M KOH. The curves present a good rectangularity indicating a good capacitive behaviour. Meanwhile, the CV plots from P-PC 1:8 to 1:11 maintain good rectangular-like shape without severe distortion at high scan rate, indicating a low equivalent series resistance and excellent capacitive properties. In particular, P-PC 1:11 shows the best rectangular-like shape even at the highest scan rate of 1000 mV/s. According to the CV curves, we deduce that these capacitors possess excellent rate capability and reversibility.

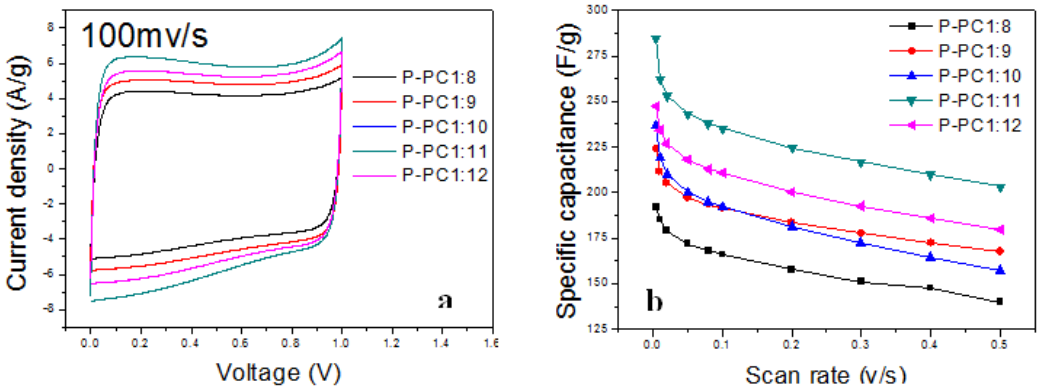

Figure 5. CV curves (a) and specific capacitances (b) of P-PC with different mass to solution volume ratios at the scan rate of 100 mV/s.

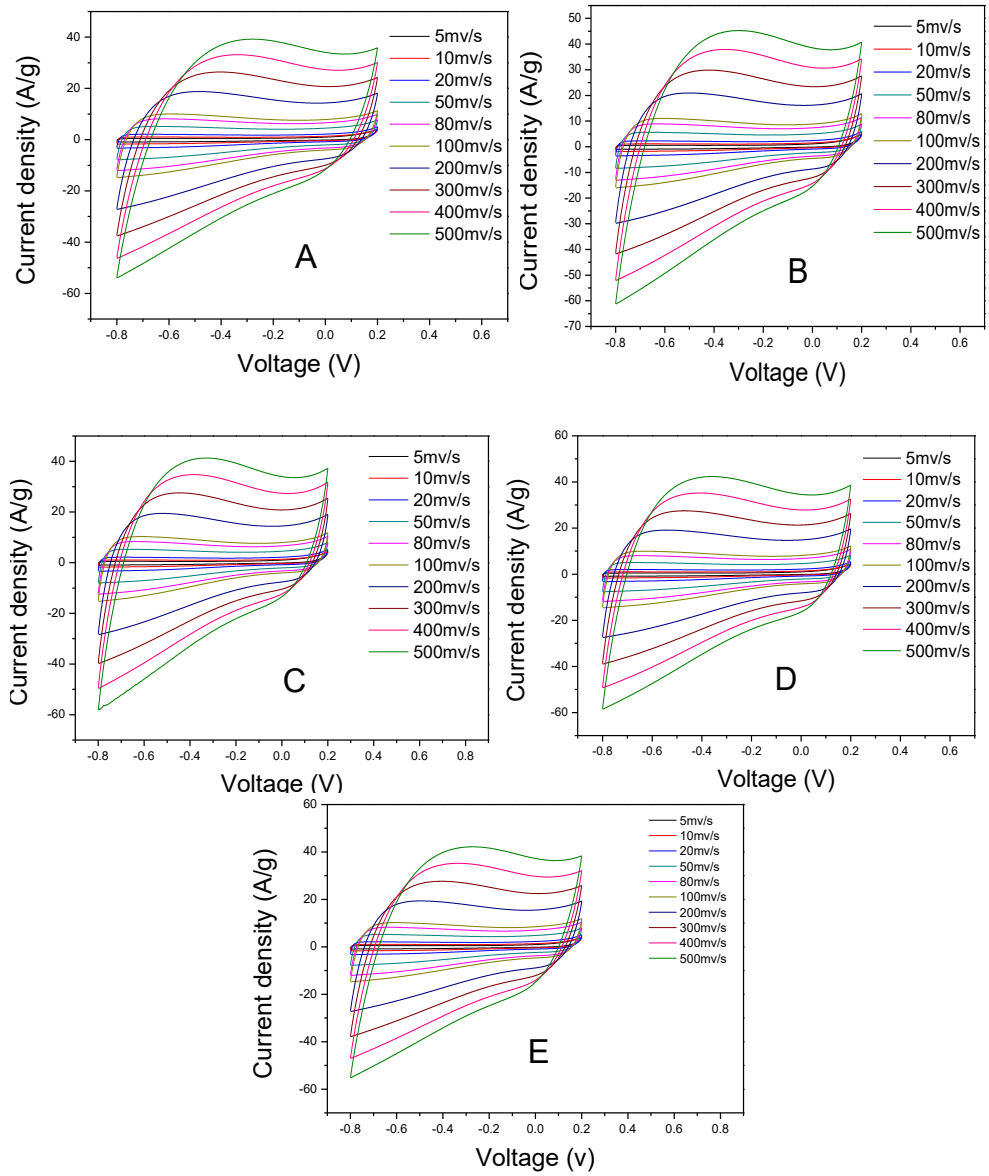

Figure 6. CV curves of N,P-PC (a) 1:1, (b) 1:2, (c) 1:3, (d) 1:4 at the scan rate between 5 and 500 mV/s carried out with three-electrode system within the operating voltage of 0.8-0.2 V in 6 M KOH electrolyte.

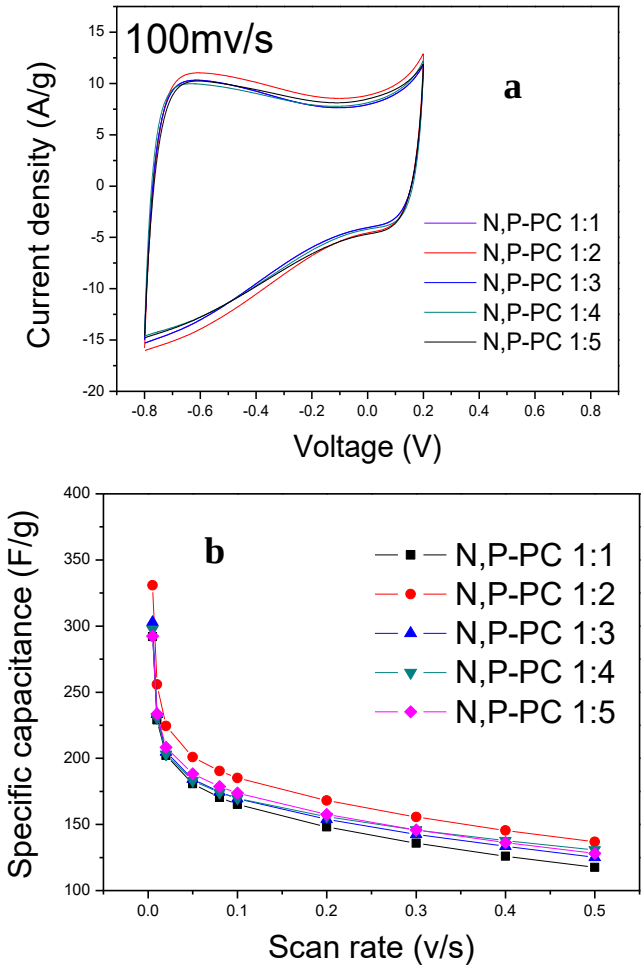

Figure 7. Electrochemical performance of N,P-PC with different doping ratio (1:1 to 1:5): (a) CV curves of N,P-PC at the scan rate of 100 mV/s, (b) the specific capacitances of N,P-PC at different scan rate (5-500 mV/s).

For further investigations, CVs from different electrodes made with different mass to solution volume ratios are acquired at the scan rate of 100 mV/s and the specific capacitance of different electrodes at different scan rate (5-500 mV/s) are derived. Interestingly, no apparent faradic process is observed in the voltage ranges of 0-1.0 V. The CV of P-PC 1:11 shows the best symmetry and highest current density suggesting the best capacitive behavior. As shown in Figure 5b, the effect of the P-doping ratio on the performance is quite obvious, namely, as the P-doping ratio increases up to 1:11, the specific capacitance increases, then it decreases. The highest specific capacitance, of P-PC (1:11), is 284.8 F/g combining both a fast ionic diffusion and a fast charge-discharge rates [5]. This is ascribed to pore size increase induced by P-doping at the PC surface [40], which may allow the electrolyte to get more easily into the pores. The results demonstrate that the optimal specific surface area and the optimum phosphorus content can sensibly affect the capacitive properties [41,42].

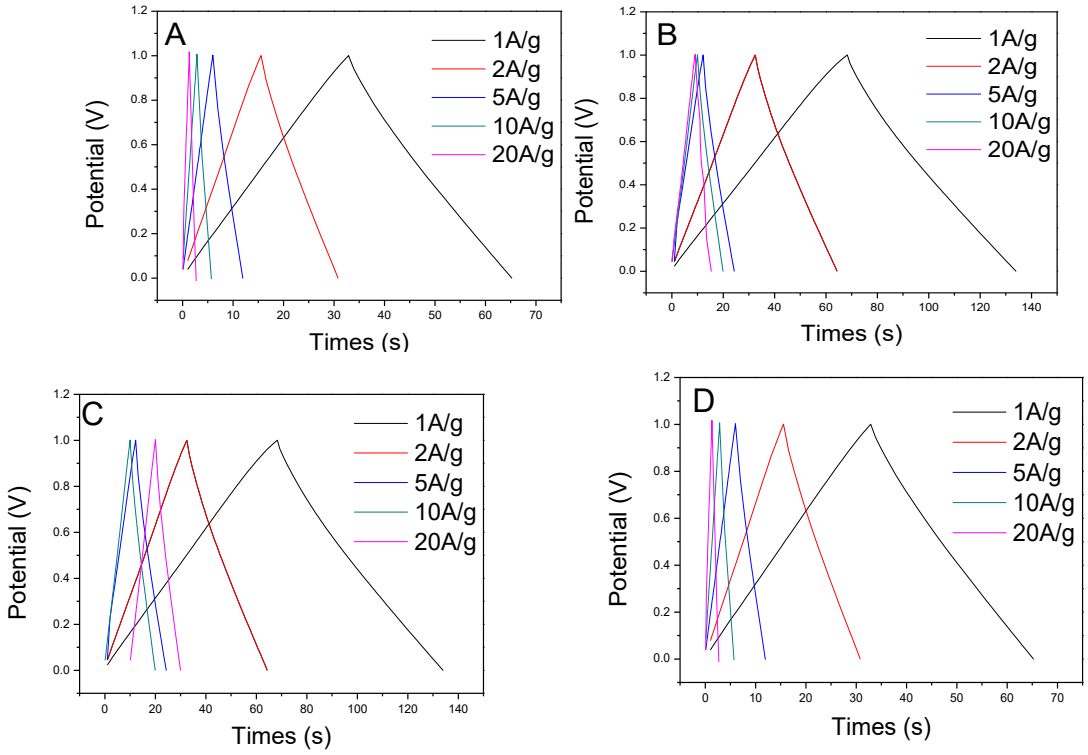

Figure 8. The GCD curves of (a) P-PC (1:11) and N,P-PCs (b) 1:1; (c) 1:2; (d) 1:3 at the current densities from 1 to 20 A/g.

Table 1. Comparison between the different heteroatom-doping carbon materials for supercapacitor electrodes.

Precursor	Activation agent	Electrolyte	C_S (F/g)	Condition	Ref.
Willow catkin	CN_2H_4S/KOH	1 M Na_2SO_4	298	0.5 A g^{-1}	[29]
	$CO(NH_2)_2$ /KOH	1 M Na_2SO_4	249	0.5 A g^{-1}	[29]
Lignosulfonate and graphene oxide	$CO(NH_2)_2$	6 M KOH	177	0.2 A g^{-1}	[24]
Black liquor-derived porous carbon	$C_3N_3(NH_2)_3$ /KOH	6 M KOH	269	0.1 A g^{-1}	[21]
Wheat straw	$C_3N_3(NH_2)_3$ /KCl /$ZnCl_2$	6 M KOH	223.9	5 mV s^{-1}	[33]
Banana peel	Thermal+NH_3	6 M KOH	210	0.5 A g^{-1}	[23]
Pomelo peel	Thermal+DHP	2 M KOH	240	0.5 A g^{-1}	[45]
Peanut shell	H_3PO_4	6 M KOH	284.8	5 mV s^{-1}	This
	H_3PO_4/ $CO(NH_2)_2$	6 M KOH	330.8	5 mV s^{-1}	work

The electrochemical performance of the N,P-PC electrode are investigated by CVs acquired in a three-electrode system at the voltage range between -0.8 and 0.2 V (Figure 6). The CVs results to be rectangular shaped and well symmetrical, with only a little deformation at high scan rate, indicating an ideal double layer capacitive behavior. The SC of N,P-PC increases and then decreases with the phosphoric activated carbon to carbamide ratio; namely, the highest SC obtained for the 1:2 ratio at the scan rate of 5 mV/s is 330.8 F/g (Figure 7). Compared to P-PC, the SC of N,P-PC presents a similar trend with the heteroatom-doping ratio increase, but at much higher values. This is ascribed to the fact that N and P doping not only provide for more electrochemically active sites but also enhance the wettability of the interface between the electrode and electrolyte [43,44]. Meanwhile, the synergistic effect of N and P doping, also give rise to a porous nanostructure with a modified surface chemistry wich may explain the higher performance [25-27,42,45]. In addition, the resulting capacitance of N-PC and N,P-PC samples in the aqueous electrolyte, is clearly higher than the most of previously reported materials which are listed in Table 1.

Galvanostatic charge/discharge cycling tests are carried of the different electrodes to explore the effect of heteroatoms (P or N, P) on the electrochemical properties of PC. Figure 8 shows the GCD curves of P-PC (1:11), N,P-PC (1:1,1:2,1:3) electrodes at the current density range between 1 and 20 A g^{-1}. Both samples show a linear and nearly symmetric profile at the current density below 5 A g^{-1}, suggesting excellent electrochemical reversibility and that the dominant contribution comes from EDLC (Electro Double Layer Capacitor). In addition, almost no IR drop is observed at the beginning of the discharge, indicating that the electrodes resistance is very small. When the current density is increased up to 10 and 20 A g^{-1}, the curves become inclined and asymmetric because of the sharp resistance increase. The SC at different current densities is given in Figure 9, showing that the SC values keep stable at low current density and decrease at high current density. Moreover, at high current density, the SC changes with the heteroatoms amount within the electrode material (Figure 9). According to the charge and discharge time and the equation $E=4I\triangle t/(m_tV)$, the SC of the N,P-PC is 119.7, 131.3 and 64.8 F/g at 1 A g^{-1}, respectively. Especially, N,P-PC 1:2 presents the highest SC of 131.3 F/g and maintains a high energy density of 18.2 Wh/Kg. These results confirm that the optimal N and P doping can sensibly promote the electrochemical performance [42].

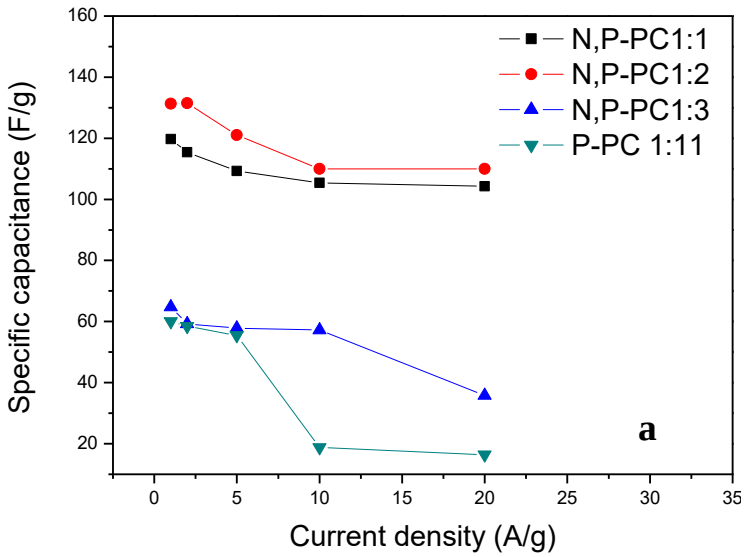

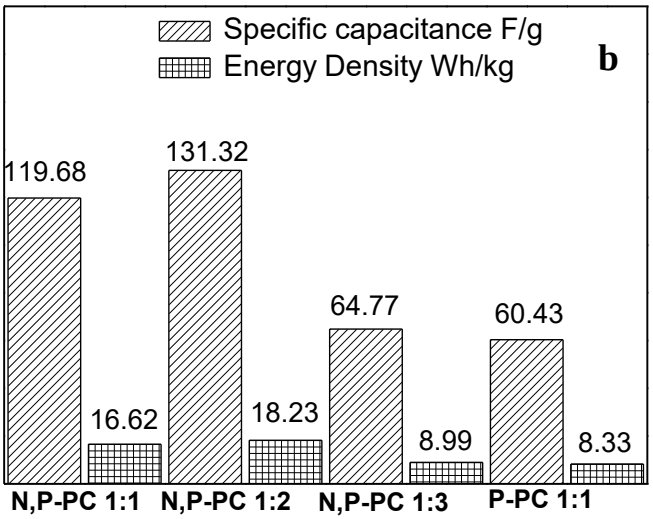

Figure 9. (a) Specific capacitance of PCs at different current density between 1 and 20 A/g. (b) Specific capacitance and energy density of PCs at the current density of 1 A/g.

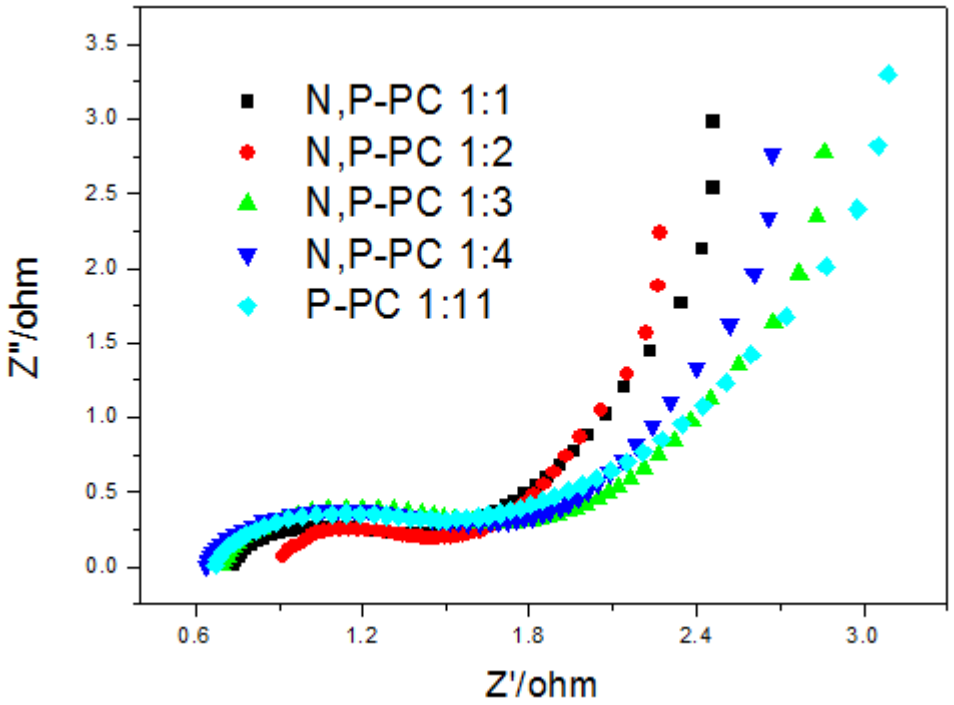

Figure 10. Nyquist plots of P-PC (1:11) and N,P-PCs.

Electrochemical impedance spectroscopy (EIS) is an important tool to investigate the electrode surface phenomena and internal reactions during the working process of electric double layer capacitors. As shown in Figure 10, the resistance values found for all electrodes are small, testifying their excellent conductivity. The verticality in low frequency region is all very high, indicating a good capacitive performance. It is also found that co-doping decreases the resistance value, meaning that N doping could improve the material's conductivity. The N,P-PC (1:2) displays the lowest resistance value, which could explain its best electrochemical performance. Overall, the results show that N,P co-

doping not only changes the architecture of the carbon material but also allows for different synergetic effects, thus enhancing the electrochemical performances of the carbon material [42,45].

4. CONCLUSIONS

Due to its low cost and facile preparation, biowaste of peanut shell was selected in this work as the carbon material source. We employed a pyrolysis followed by the activation to provide for P and N,P-co-doping to convert peanut shell into heteroatom-doped porous carbon structures. Both the P and N doping contributed to the enhancement of the specific capacitance in the KOH. In addition, N,P co-doping allows for synergetic effects promoting the capacitor performance. Especially, N,P-PC (1:2) presented the highest SC of 330.8 F/g at the scan rate of 5 mV s^{-1} while the energy density was 18.2 Wh/Kg. This work demonstrates a facile method to fabricate porous carbons from waste biomass, which may have potential applications in many fields, such as adsorption, catalysis and energy storage.

ACKNOWLEDGMENTS
This research thanked the supporting of the National Science Foundation of China (51603147) and Tianjin application foundation and advanced technology research plan project (14RCHZGX00859).

References

1. P. Simon, Y. Gogotsi, *Nat. Mater.,* 7 (2008) 845.
2. E. Perricone, M. Chamas, J.C. Leprêtre, P. Judeinstein, P. Azais, E.R. Pinero, F. Béguin, F. Alloin, *J. Power Sources*, 239 (2013) 217.
3. C. Lei, N. Amini, F. Markoulidis, P. Wilson, S. Tennisonb, C. Lekakou, *J. Mater. Chem. A,* 1 (2013) 6037.
4. M. Winter, R.J. Brodd, *Chem. Rev.*, 35 (2004) 4245.
5. L.L. Zhang, X.S. Zhao , *Chem. Soc. Rev.,* 38 (2009) 2520.
6. P. Simon, Y. Gogotsi, *Nat. Mater.,* 7 (2008) 845.
7. X.W. Yu, D.B. Ruan, C.C.Wu, J.Wang, Z.Q. Shi, *J. Power Sources*, 265 (2014) 309.
8. F. Cheng, X.W. Yu, J.Wang , Z.Q. Shi, C.C.Wu, *Electrochim. Acta*, 200 (2016) 106.
9. J. Wang, L.Shen, B.Ding, P.Nie, H.Deng, H.Dou, X.Zhang, *RSC Adv.*, 4 (2014) 7538.
10. A.G. Pandolfo, A.F. Hollenkamp, *J. Power Sources*, 157 (2006) 11.
11. H. Wang, Z. Xu, A. Kohandehghan, Z. Li, K. Cui, X. Tan, T.J. Stephenson, C.K. King'ondu, C.M. Holt, B.C. Olsen, *ACS Nano*, 7 (2013) 5131.
12. C.X. Guo, C.M. Li, *Energy Enviro. Sci.,* 4 (2011) 4504.
13. Z. Yu, L. Tetard, L. Zhai, J. Thomas, *Energy Enviro. Sci.,* 8 (2015) 702.
14. Z. Yan, Z.Peng, J.M. Tour, *Acc.Chem.Res.,* 47 (2014) 1327.
15. Y. Li, K. Ye, K. Cheng, J. Yin, D. Cao, G. Wang, *J.Power Sources*, 274 (2015) 943.
16. Z. Xing, B.Wang, J.K. Halsted, R. Subanshchandrabose, W.F. Stickle, X. Ji, *Chem. Commun.,* 51 (2015) 1969.
17. M. Lotya, Y. Hernandez, P.J. King, R.J. Smith, V. Nicolosi, L.S. Karlsson, F.M. Blighe, S. De, Z. Wang, I. McGovern, *J. Am. Chem. Soc.*,131 (2009) 3611.
18. B. Subramanya, D.K. Bhat, *New J. Chem.*,39 (2015) 420.
19. M. Lee, G.P. Kim, H.D. Song, S. Park, J. Yi, *Nanotech.,* 25 (2014) 345601.
20. Z. Li, L. Zhang, B.S. Amirkhiz, X. Tan, Z. Xu, H. Wang, B.C. Olsen, C. Holt, D. Mitlin, *Adv. Energy Mater.*,2 (2012) 431.
21. L.F. Zhu, F. Shen, R.L. Smith Jr, L.L. Yan, L.Y. Li, X.H. Qi, *Chem. Eng. J.*, 316 (2017) 770.

22. L. Chen, Y.Z. Zuo, Y. Zhang, Y.M. Gao, *Int. J. Electrochem. Sci.*, 13(2018) 642.
23. B.Z. Liu, L.L. Zhang, P.R. Qi, M.Y. Zhu, G. Wang, Y.Q. Ma, *Nanomaterials*, 6 (2016) 18.
24. H.B. Zhao, W.D. Wang, Q.F. Lu, T.T. Lin, Q.L. Lin, H.J. Yang, *Bioresour. Technol.*, 176 (2015) 106.
25. P.F. Fulvio, J.S. Lee, R.T. Mayes, X. Wang, S.M. Mahurin, S. Dai, *Phys. Chem. Chem. Phys.* ,13 (2011) 13486.
26. S. Wang, E. Iyyamperumal, A. Roy, Y. Xue, D. Yu, L. Dai, *Angew.Chem. Int. Ed.*, 50 (2011) 11756.
27. D. Hulicova-Jurcakova, M. Seredych, G.Q. Lu, N. Kodiweera, P.E. Stallworth, S. Greenbaum, T.J. Bandosz, *Carbon* ,47 (2009) 1576.
28. J. Xu, G. Dong, C. Jin, M. Huang, L. Guan, *ChemSusChem*, 6 (2013) 493.
29. Y.J. Li, G. L. Wang, T. Wei, Z. J. Fan, P. Yan, *Nano Energy* 19 (2016) 165.
30. S. Wang, E. lyyamperumal, A. Roy, Y. Xue, D. Yu, L. Dai, *Angew. Chem. Int. Ed.*, 50 (2011) 11756.
31. J. Zhu, P. Shen, *RSC Adv.*, 3 (2013) 14686.
32. Y. Zhou, R.G. Ma, Stephanie L. Candelaria, J.C. Wang, Q. Liu, E. Uchaker, P.X. Li, Y.F. Chen, G.Z. Cao, *J.Power Sources*, 314 (2016) 39.
33. S. Zhang, K. Tian, B.H. Cheng, H. Jiang, *ACS Sustainable Chem. Eng.*, 5 (2017) 6682.
34. N. Guo, M. Li, X. Sun, F. Wang, R. Yang, *Green Chem.*, 19 (2017) 2595.
35. Y. Fan, P.F. Liu, Z.Y. Huang, T.W. Jiang, K.L. Yao, R. Han, *J. Power Sources*, 280 (2015) 30
36. J. Yi, Y. Qing, C. Wu, Y. Zeng, Y. Wu, X. Lu, Y. Tong, *J. Power Sources*, 351 (2017) 130.
37. B. Li, F. Dai, Q. Xiao, L. Yang, J. Shen, C. Zhang, M. Cai, *Energy Environ. Sci.*, 9 (2016) 102.
38. J. Jin, X. Qiao, F. Zhou, Z.S. Wu, L. Cui, H. Fan, *ACS Appl. Mater. Interfaces*, 9 (2017) 17317.
39. Z. Tian, M. Xiang, J. Zhou, L. Hu, J. Cai, *Electrochim. Acta*, 211 (2016) 225.
40. Q.S. Liu, T. Zheng, P. Wang, L. Guo, *Ind. Crop. Prod.*, 31 (2010) 233.
41. Raymundo-Piñero, F. Leroux, F. Béguin, *Adv. Mater.*, 18 (2006) 1877
42. J. Chen, H.M. Wei, H.J. Chen, W.H. Yao, H.L. Lin, S. Han, *Electrochim. Acta*, 271 (2018) 49.
43. X. Yu, H.J. Kim, J.Y. Hong, Y.M. Jung, K.D. Kwon, J. Kong, *Nano Energy*, 15 (2015) 576.
44. X.Y. Chen, C. Chen, Z.J. Zhang, D.H. Xie, X. Deng, J.W. Liu, *J. Power Sources*, 230 (2013) 50.
45. Z. Wang, Y.t. Tan, Y.L. Yang, X.N. Zhao, Y. Liu, L.Y. Niu, B. Tichnell, L.B. Kong, L. Kang, Z. Liu, F. Ran, *J. Power Sources*, 378 (2018) 499.